

Simultaneous Segmentation of Range and Color Images Based on Bayesian Decision Theory

Pierre Boulanger
Department of Computing Science
University of Alberta
PierreB@cs.ualberta.ca

Abstract

This paper describe a new algorithm to segment in continuous parametric regions registered color and range images. The algorithm starts with an initial partition of small first order regions using a robust fitting method constrained by the detection of depth and orientation discontinuities in the range signal and color edges in the color signal. The algorithm then optimally group these regions into larger and larger regions using parametric functions until an approximation limit is reached. The algorithm uses Bayesian decision theory to determine the local optimal grouping and the complexity of the parametric model used to represent the range and color signals. Experimental results are presented.

1. Introduction

The ability to integrate and represent in a coherent manner multiple source of sensor data is at the base of understanding images in terms of intrinsic physical properties. This paper describe a method to segment range and color data produced by color range sensor [11] or by a combination of color cameras and range sensors [15]. Many of these sensors can measure in perfect registration a range signal corresponding to the distance between the sensor and the surface of an object and a corresponding color signal which is proportional to the reflectivity of the surface at this point.

Many references to the problem of sensor fusion can be found in the literature. A survey and analysis of multi-sensor fusion and integration methods can be found in Luo and Kay [9], Allen et al. [1], and Stamos and Allen [15].

Hackett and Shan [7] segment range and intensity images by using a split and merge method. The algorithm consist of two steps. First, the initial seed regions are determined by using the most dominant sensor at a given time. Second, the initial segmentation is refined by using region

merging based on if the strength of range and intensity boundaries are low.

In the case of color and range sensor fusion very few paper can be found. Baribeau et al. [2] discuss the problem of estimating the bidirectional reflectance-distribution function (BRDF) for each pixel from the fusion of the range and color information and a sensor model. Shirai [14] integrate sparse range data obtained by stereo vision with color data, using color stereo pair. The color is used to assist in model-based classification and object recognition to build a rich description of the scene. Regions are first classified using color and further split based on edge information and range information obtained from stereo. The scene is eventually represented in a series of 3-D planar patches and its relationship between them. Rushmeier et al. [13] try to compute the Bi-directional Reflectance Function of colored objects using the normals computed from the range data.

In this paper, one will analyze a new segmentation algorithm based on a hierarchical grouping of an initial partition based on a Bayesian criteria. The algorithm starts with an initial partition of the range and color images constrained by the detection of depth and orientation discontinuities in the range image and of color edges in the corresponding color image.

From this initial partition, the algorithm start grouping these regions into larger and larger one until the approximation error in one of the region is greater than a pre-determined threshold. The algorithm then try to transform these primitives into more complex ones by using higher order parametric models. The key idea behind the algorithm is that one should start with the simplest hypothesis about the model of the data, and gradually increase the complexity of the hypothesized form as statistical evidence grows. This paper present a consistent view of the grouping criterion and of the generalization process based on Bayesian decision framework. The end result of this segmentation process is a compact representation of a scene composed of continuous surface patches with a constant parametric color model.

2. Problem Definition

In this approach to segmentation, the relevant structure of a range and color image is viewed as a piecewise smooth parametric polynomial contaminated by noise. A piecewise smooth parametric surface $\vec{\eta}_r(u, v)$ and its corresponding color signal $\vec{\eta}_c(u, v)$ can be partitioned into N smooth surface models $\vec{f}_{rl}(u, v; \mathbf{A}_{rl})$ and color models $\vec{f}_{cl}(u, v; \mathbf{A}_{cl})$ over a connected support region Ω_l :

$$\vec{\eta}_r(u, v) = \sum_{l=1}^N \vec{f}_{rl}(u, v; \mathbf{A}_{rl}) \xi(u, v, \Omega_l) \quad (1)$$

$$\vec{\eta}_c(u, v) = \sum_{l=1}^N \vec{f}_{cl}(u, v; \mathbf{A}_{cl}) \xi(u, v, \Omega_l) \quad (2)$$

where $\xi(u, v, \Omega_l)$ is the characteristic function of the region Ω_l , and is equal to one if $(u, v) \in \Omega_l$ and zero otherwise. The arrays \mathbf{A}_{rl} and \mathbf{A}_{cl} are the model parameters for each signal. The function $\vec{\eta}_r(u, v) = (x, y, z)^T$ is a three dimensional signal corresponding to the x, y, z component of the range signal and the function $\vec{\eta}_c(u, v) = (r, g, b)^T$ to the red r , green g , and blue b component of the color signal.

The segmentation problem can be stated as following: given a discrete range $\vec{r}(u_i, v_i) = (x_i, y_i, z_i)^T$ and color image $\vec{C}(u_i, v_i) = (r_i, g_i, b_i)^T$ and an approximation thresholds ε_t find the N image regions Ω_l approximated by N statistically reliable functions $\vec{f}_{rl}(u_i, v_i; \mathbf{A}_{rl})$ and $\vec{f}_{cl}(u_i, v_i; \mathbf{A}_{cl})$ subject to:

$$\chi^2 = \frac{1}{n_l} \sum_{(u_i, v_i) \in \Omega_l} (\vec{f}_{rl} - \vec{r})^T \Sigma_r^{-1} (\vec{f}_{rl} - \vec{r}) + (\vec{f}_{cl} - \vec{C})^T \Sigma_c^{-1} (\vec{f}_{cl} - \vec{C}) < \varepsilon_t \quad \forall l = 1, \dots, N \quad (3)$$

The parameter n_l is equal to the number of pixels in the region Ω_l . The matrices Σ_r and Σ_c are the covariance matrices of the noise associated to the range and color signal and can be modelled using a technique described in [10].

The basic steps of the algorithm are the following:

1. Normalize the color by computing the bidirectional reflectance- distribution function (BRDF) at each pixel.
2. Do an initial partitioning of the data set based on a first order parametric model using a robust fitting technique constrained by depth and orientation discontinuities in the range signal and color edges in the corrected color signal.
3. Group adjacent first order regions with other first order regions or points to produce a larger first order region. Validate the grouping corresponding to the one which is the most similar based on a Bayesian criterion.

4. Loop until the similarity criterion is smaller than a pre-determined threshold.
5. Generalize the first order regions to second order one if the decision is supported by statistical significance test.
6. Group adjacent first or second order regions to other points, first, or second order regions to produce a larger region corresponding to the highest order of the two. Validate the grouping corresponding to the one which is the most similar.
7. Generalize second order regions into higher order parametric polynomials using geometrical heuristics if it is supported by Bayesian decision.
8. Proceed with more grouping until no more regions are generalized.

3. Color Reflectance Modelling

Ideally the color signal should be independent of the sensor parameters and should depend only on basic physical properties such as the material pigmentation. Baribeau et al. [2] and later [13] discuss such possibilities by modelling the physical image formation of the color range sensor using a Lambertian model. Using a similar physical model, the total power received at the detector at time t is equal to:

$$P_r(u, v; \lambda) = \left(\frac{1}{4\pi} S_r T_r \exp(-\alpha r) T_x P_x(u, v; \lambda) \right) \times \left(\frac{\rho_\lambda(u, v) \vec{\mu} \cdot \vec{n}(u, v)}{r^2} \right) \quad (4)$$

where $P_x(u, v; \lambda)$ is equal to the instantaneous total power of the transmitted laser in the direction $\vec{\mu}$ and a wavelength λ ; T_x is the transmission coefficient of the incident beam; T_r is the transmission coefficient of the reflected signal produced by a Lambertian surface of area S_r with a normal equal to $\vec{n}(u, v)$ and an albedo equal to $\rho_\lambda(u, v)$ at a distance r from the measuring sensor; α is the coefficient of attenuation in the atmosphere and is assumed constant for all wavelength used. The relative power between the incident beam and the measured one is equal to:

$$\frac{P_r(u, v, t; \lambda)}{P_x(u, v; \lambda)} = K \left(\frac{\rho_\lambda(u, v) \vec{\mu} \cdot \vec{n}(u, v)}{r^2} \right) \quad (5)$$

where $K = \frac{1}{4\pi} S_r T_r \exp(-\alpha r) T_x$ and is assumed to be a constant for all wavelength. An estimate of the incident laser power $P_w(u, v, \lambda)$ can be performed by scanning a white Lambertian surface for each similar u, v . The power is equal to:

$$P_x(u, v; \lambda) = \frac{r_w^2 P_w(u, v, \lambda)}{\vec{n}_w(u, v) \cdot \vec{\mu}} \quad (6)$$

Using this estimated laser power one can compute the **bidirectional reflectance distribution function (BRDF)** with the following equation:

$$\frac{P_r(u, v, t; \lambda)}{P_x(u, v; \lambda)} \left(\frac{r^2}{\vec{\mu} \cdot \vec{n}(u, v)} \right) = \rho_\lambda(u, v). \quad (7)$$

The white standard used as a reference is a mat bar coated with barium sulphite paint. This material is known to have very good Lambertian behavior. The computed BRDF for the three wavelength is an intrinsic property corresponding to the material pigmentation. More detail on how to calibrate the system and estimate the various unknown parameters can be found in [2].

4. Multidimensional Signal Representation

The type of model used to represent the shape of the range data and the spatial evolution of the intrinsic color is highly constrained by the feasibility of the corresponding segmentation algorithm. A parametric Bézier polynomial is used to represent both signals and is defined as:

$$\vec{f}_{sl}(u, v; \mathbf{A}_{sl}) = \sum_{i=0}^k \sum_{j=0}^k \vec{a}_{ij} B_i(u) B_j(v) \quad (8)$$

$B_m(t)$ is a Bernstein polynomial defined as:

$$B_m(t) = \frac{k!}{(k-m)!m!} t^m (1-t)^{k-m}. \quad (9)$$

The subscript s can be equal to r or c depending on if one wants to represent the range or color information. This equation can be represented in matrix form by:

$$\vec{f}_{sl}(u, v; \mathbf{A}_{sl}) = \mathbf{A}_{sl} \mathbf{M}_{l|uv} \quad (10)$$

where the array $\mathbf{A}_{sl} = [\vec{a}_{00}, \vec{a}_{10}, \vec{a}_{01}, \dots, \vec{a}_{kk}]$ is the coefficients array of size $3 \times (k+1)^2$ and

$$\mathbf{M}_{l|uv} = [B_0(u)B_0(v), B_1(u)B_0(v), B_0(u)B_1(v), \dots, B_k(u)B_k(v)]^T \quad (11)$$

is the basis function matrix of size $(k+1)^2 \times 1$.

If one assume that the range $\vec{r}(u_i, v_i)$ and color $\vec{C}(u_i, v_i)$ image data is corrupted by Gaussian noise of means $\vec{\mu}_r = \vec{\mu}_c = \vec{0}$ and for which the covariance matrices are equal to Σ_r and Σ_c , then the optimal model coefficients are the ones which minimize the log-likelihood function of the observations corresponding to the minimum of the standard least squared metric L^2 given by equation (3).

The minimum occurs when $\nabla_{\mathbf{A}_{rl}} \chi^2 = 0$ and $\nabla_{\mathbf{A}_{cl}} \chi^2 = 0$ which correspond in matrix form to:

$$\mathbf{T}_{sl} = \mathbf{A}_{sl} \mathbf{L}_l \quad (12)$$

where $\mathbf{L}_l = [\mathbf{M}_{l|u_1 v_1}, \dots, \mathbf{M}_{l|u_{n_l} v_{n_l}}]$ is a matrix of size $(k+1)^2 \times n_l$ and $\mathbf{T}_{sl} = [\vec{s}(u_1, v_1), \dots, \vec{s}(u_{n_l}, v_{n_l})]$ a matrix of size $3 \times n_l$ corresponding to the sensor measurements. The solution correspond to the normal equation equal to:

$$\mathbf{A}_{sl} = \mathbf{T}_{sl} \mathbf{L}_l^T (\mathbf{L}_l \mathbf{L}_l^T)^{-1} = \mathbf{V}_{sl} \mathbf{R}_l^{-1} \quad (13)$$

where \mathbf{R}_l is an Hermitian matrix of size $(k+1)^2 \times (k+1)^2$ corresponding to the covariance matrix of the basis functions and \mathbf{V}_{sl} is a matrix corresponding to the correlation between the basis functions and the measurements. Using this notation the covariance matrix of the approximation error is equal to:

$$\hat{\Sigma}_{sl} = \mathbf{T}_{sl} \mathbf{T}_{sl}^T - 2 \mathbf{A}_{sl} \mathbf{V}_{sl}^T + \mathbf{A}_{sl} \mathbf{R}_l \mathbf{A}_{sl}^T \quad (14)$$

The average error on the model parameters $\delta \mathbf{A}_l$ is proportional to the diagonal element of the inverse of the matrix \mathbf{R}_l , i.e.,

$$\delta \mathbf{A}_{sl} = \frac{\mathbf{D}_{sl}^T \mathbf{U}_l}{n_l - (k-1)^2} = [\delta \mathbf{A}_{sl|i}, \delta \mathbf{A}_{sl|j}, \delta \mathbf{A}_{sl|k}]^T \quad (15)$$

where $\mathbf{D}_l = [\text{Diag } \hat{\Sigma}_{sl}] = [\hat{\sigma}_{sl|i}^2, \hat{\sigma}_{sl|j}^2, \hat{\sigma}_{sl|k}^2]$ is a 1×3 matrix corresponding to the variance of the fitting error in each orthogonal directions and is equal to the diagonal elements of the matrix $\hat{\Sigma}_{sl}$. The matrix $\mathbf{U}_l = [\text{Diag } \mathbf{R}_l^{-1}]$ is a $1 \times (k+1)^2$ matrix where each element is the diagonal element of the covariance matrix \mathbf{R}_l^{-1}

5. Initial Partition Method

Like many region growing techniques, one needs to make an initial guess of the primitives and then iteratively refine the solution. Besl [3] used the topographic map based on the sign of Gaussian and mean curvatures to determine seed points where his algorithm grows regions of increasing size and complexity from. There is a relationship between the quality of the initial guess and the number of iterations required to converge to the final region size. Because of the importance of the initial partition, the algorithm use a robust fitting technique constrained by previously detected depth and orientation discontinuities in the range image and edges in the color image. The algorithm uses a Least Median Square (LMS) fitting method first described by Rousseeuw and Leroy [12] which allows a robustness up to 50% outliers. The algorithm to find the initial partition is the following:

- Set the window size $L = L_{\max}$ to the maximum window size (typically 11×11).
- Find a square neighborhood of size $L \times L$ where there is no depth nor orientation discontinuities nor color edges present.

- Do least median square fitting and detect the outliers (not sensitive to 50% of outliers).
- Eliminate the outlier from the window by releasing their availability to be used by other regions.
- Compute the least square model without the outliers for the range and color information.
- Proceed for the whole image with the same window size.
- Do the same operation with a reduced window size $L = L - 2$ until the minimum window size L_{\min} has been reached (typically 3×3).

This new initial partition technique is not sensitive to impulse noise (up to 50% of outliers) and is capable of producing excellent seed regions even for a large neighborhood.

6. Compatibility Function

A similarity function is a predicate that determine if two regions can be merged into one. Let Ω_i be a region composed of n_i points defined by the maximum likelihood model parameters $\mathbf{A}_{ri} = (\vec{b}_{00}, \vec{b}_{10}, \dots, \vec{b}_{kk})^T$ for the range signal and $\mathbf{A}_{ci} = (\vec{c}_{00}, \vec{c}_{10}, \dots, \vec{c}_{kk})^T$ for the color signal. Each region is also characterized by their covariance matrices $\hat{\Sigma}_{ri}$ and $\hat{\Sigma}_{ci}$. Let $\delta\mathbf{A}_{ri} = (\delta\vec{b}_{00}, \delta\vec{b}_{10}, \dots, \delta\vec{b}_{kk})^T$ and $\delta\mathbf{A}_{ci} = (\delta\vec{c}_{00}, \delta\vec{c}_{10}, \dots, \delta\vec{c}_{kk})^T$ be the margin of error on the model parameters estimated by equation (15). Let $\{\Omega_m\}$ be the set of N_t regions adjacent to the region Ω_i and defined by the models \mathbf{A}_{rm} and \mathbf{A}_{cm} with a margin of error equal to $\delta\mathbf{A}_{rm}$ and $\delta\mathbf{A}_{cm}$. The best grouping of region Ω_i with one of its neighbors correspond to the one for which:

$$P(\Omega_b \wedge \Omega_i | \Omega_i) = \max_b \frac{\prod_{u,v \in \Omega_i} p_t(u, v | \mathbf{A}_{rb}; \mathbf{A}_{cb}) p(\delta\mathbf{A}_{rb}) p(\delta\mathbf{A}_{cb})}{\sum_{j=1}^{N_t} \prod_{u,v \in \Omega_i} p_t(u, v | \mathbf{A}_{rj}; \mathbf{A}_{cj}) p(\delta\mathbf{A}_{rj}) p(\delta\mathbf{A}_{cj})} \quad (16)$$

where $p_t(u, v | \mathbf{A}_{rb}; \mathbf{A}_{cb})$ is equal to the probability that a point in region Ω_i with coordinate u and v would be predicted by one of the models \mathbf{A}_{rb} and \mathbf{A}_{cb} adjacent to Ω_i . The likelihood of grouping the region Ω_i with Ω_b is given by:

$$\begin{aligned} P(\Omega_i | \mathbf{A}_{rb}; \mathbf{A}_{cb}) &= \alpha \exp\left(-\frac{\hat{\sigma}_{ib}^2}{2}\right) \\ &= \prod_{u,v \in \Omega_i} p_t(u, v | \mathbf{A}_{rb}; \mathbf{A}_{cb}) \end{aligned} \quad (17)$$

where

$$\hat{\sigma}_{ib}^2 = \text{Tr}[(\mathbf{T}_{ri} \mathbf{T}_{ri}^T - 2\mathbf{A}_{rb} \mathbf{V}_{ri}^T + \mathbf{A}_{rb} \mathbf{R}_{ri} \mathbf{A}_{rb}^T) \Sigma_r^{-1} + (\mathbf{T}_{ci} \mathbf{T}_{ci}^T - 2\mathbf{A}_{cb} \mathbf{V}_{ci}^T + \mathbf{A}_{cb} \mathbf{R}_{ci} \mathbf{A}_{cb}^T) \Sigma_c^{-1}] \quad (18)$$

is the sum of the square difference between the functions representing region Ω_b extrapolated to predict region Ω_i . The functions $p(\delta\mathbf{A}_{rb})$ and $p(\delta\mathbf{A}_{cb})$ is the *a priori* probability of the region Ω_b and can be evaluated by the following equation:

$$\begin{aligned} p(\delta\mathbf{A}_{rb}) &= \omega_1 \exp\left[-\frac{1}{2} [\delta\mathbf{A}_{rb|x} \Sigma_{Ar}^{-1} \delta\mathbf{A}_{rb|x}^T \right. \\ &\left. + \delta\mathbf{A}_{rb|y} \Sigma_{Ar}^{-1} \delta\mathbf{A}_{rb|y}^T + \delta\mathbf{A}_{rb|z} \Sigma_{Ar}^{-1} \delta\mathbf{A}_{rb|z}^T] \right] \end{aligned} \quad (19)$$

$$\begin{aligned} p(\delta\mathbf{A}_{cb}) &= \omega_2 \exp\left[-\frac{1}{2} [\delta\mathbf{A}_{cb|r} \Sigma_{Ac}^{-1} \delta\mathbf{A}_{cb|r}^T \right. \\ &\left. + \delta\mathbf{A}_{cb|g} \Sigma_{Ac}^{-1} \delta\mathbf{A}_{cb|g}^T + \delta\mathbf{A}_{cb|b} \Sigma_{Ac}^{-1} \delta\mathbf{A}_{cb|b}^T] \right] \end{aligned} \quad (20)$$

where Σ_{Ar} and Σ_{Ac} are equal to the true covariance matrix of the parameters \mathbf{A}_{rb} and \mathbf{A}_{cb} and represents the strength of the belief that the coefficients of the matrices \mathbf{A}_{rb} and \mathbf{A}_{cb} are the true value of the coefficients. In practice, the covariance matrix cannot be evaluated, but in our implementation, we artificially set the diagonal elements of the matrix Σ_{Ar} and Σ_{Ac} are equal to β^2 and the off-diagonal to zero.

From equations (18), (19), and (20) the *a posteriori* probability of a grouping correspond to the one which maximize the numerator. If one compute the log of the numerator of equation (17), one obtain a grouping coefficient equal to:

$$\begin{aligned} c_{ib} &= \hat{\sigma}_{ib}^2 + \frac{(\hat{\sigma}_{rb|x}^2 + \hat{\sigma}_{rb|y}^2 + \hat{\sigma}_{rb|z}^2) \text{Tr} \mathbf{R}_{rb}^{-1}}{\beta^2(n_b - (k-1)^2)} + \\ &\frac{(\hat{\sigma}_{cb|r}^2 + \hat{\sigma}_{cb|g}^2 + \hat{\sigma}_{cb|b}^2) \text{Tr} \mathbf{R}_{cb}^{-1}}{\beta^2(n_b - (k-1)^2)} \end{aligned} \quad (21)$$

Using this compatibility coefficient, one can select the best groupings, by selecting from all the possible grouping the one corresponding to the minimum value.

7. Geometrical Generalization

The problem of segmentation is to find the most reliable minimal description of an image. This statement implies that the complexity of the model used by the segmentation algorithm must only be increased if there is a strong statistical evidence. Let $\hat{\sigma}_t^2$ be the approximation error of the model with the larger number of parameters $p_{\max} = (k+1)^2$ as computed by equation (13). Its value is kept as a comparison basis. In order to validate a parameter in one of the coefficient matrices \mathbf{A}_{ri} and \mathbf{A}_{ci} the algorithm first eliminate this element from the coefficient matrix by setting it equal to zero and then compute the new approximation error $\hat{\sigma}_n^2$. The variation of the relative error is given by:

$$\frac{\hat{\sigma}_n^2 - \hat{\sigma}_t^2}{\hat{\sigma}_t^2} = \frac{\hat{\sigma}_n^2}{\hat{\sigma}_t^2} - 1 = r - 1. \quad (22)$$

The variables $\hat{\sigma}_n$ and $\hat{\sigma}_t$ are equal to the sum of the squared error for the reduced model and the full model respectively.

If the statistics r is close to unity, one may conclude with confidence that the i^{th} component of one of coefficient matrices is not statistically significant. The statistical distribution of the variable r is distributed as a Snedecor's F distribution with $\nu_1 = 1$ and $\nu_2 = n_l - p_{\max}$ degrees of freedom. The decision to reject the parameter i from the coefficient matrix with a degree of confidence α is given by:

$$P_F(r \geq r_o) = \int_{r_o}^{\infty} p_F(r) dr \geq \alpha. \quad (23)$$

In the algorithm the parameter α is set equal to 0.1.

8. Experimental Results

In order to illustrate the segmentation process, a billiard ball composed of different color region was scanned using the National Research Council color range sensor. One can see in Figure 1a a 3-D display of the color range image. In the present implementation, the position of depth and orientation discontinuities and color edges was computed by using a morphological method developed by Boulanger [4]. One can see in Figure 1b the combined range and color edges. After the initial partition of the scene and the generation of the graph structure to represent this partition, the algorithm start the grouping process as described above. The grouping process is terminated when the average extrapolation error $\hat{\sigma}_{ib}$ of the best grouping is over a threshold of 0.5 mm in the range image and 10.0 in the color image. The model generalization method is then applied and the grouping process resumed for the same threshold. One can see in Figure 1c the partition of the scene produced by the algorithm and in Figure 1d the reconstructed color range image from the segmentation model. A similar segmentation process was applied to a series of color band applied with a wide paint brush. One can see in Figure 2a the range and color image of the painting and in Figure 2b the resulting label map for a grouping threshold of 1.0 mm in the range image and 20.0 in the color image. One can see in Figure 2c the reconstructed color range image from the segmentation parameters.

9. Conclusion

The present algorithm produce a quasi-optimal partition of colored range images even when the images are corrupted by a high level of noise. At the end of the hierarchical grouping, one has a model where one can analyze color range images at different levels of representation. The data structure produced by the algorithm is directly accessible to high level tasks such as model building, identification, and pose determination. The algorithm is also clean in

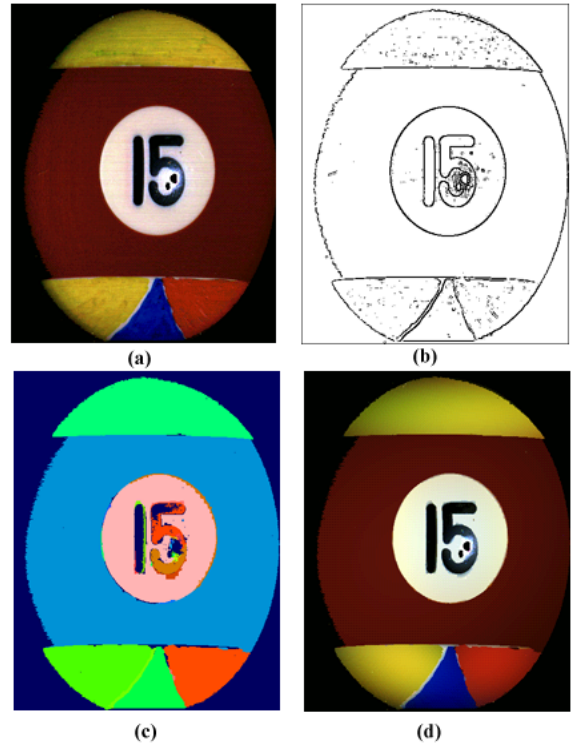


Figure 1. Segmentation of color range images of a billiard ball: (a) 3-D view of the color range image (b) detected range and color edges, (c) segmented image regions, (d) reconstructed color range image.

the sense that there is no ad-hoc threshold (beside resolution ε_t and the *a priori* distribution parameter β) that would make the algorithm hard to tune. Bayesian decision criterion always makes sure that one take the best grouping or generalization decision.

References

- [1] P. Allen, I. Stamos, A. Gueorguiev, E. Gold, and P. Blaser, *AV-ENUE: Automated Site Modeling in Urban Environment*, hird Conference on 3D Digital Imaging and Modeling, Quebec, Canada, May 28th-June 1st, 2001.
- [2] R. Baribeau, M. Rioux, and G. Godin, *Color reflectance modeling using a polychromatic laser range sensor*, IEEE Trans. on Pattern Analysis and Machine Intelligence, Vol. PAMI-14, no. 2, pp. 263-269, 1992.
- [3] P.J. Besl and R.C. Jain, *Segmentation through variable-order surface fitting*, IEEE Trans. on Pattern Analysis and Machine Intelligence, Vol. PAMI-10, no. 2, pp. 167- 192, 1988.
- [4] P. Boulanger, F. Blais, and P. Cohen, *Detection of depth and orientation discontinuities in range images using mathemat-*

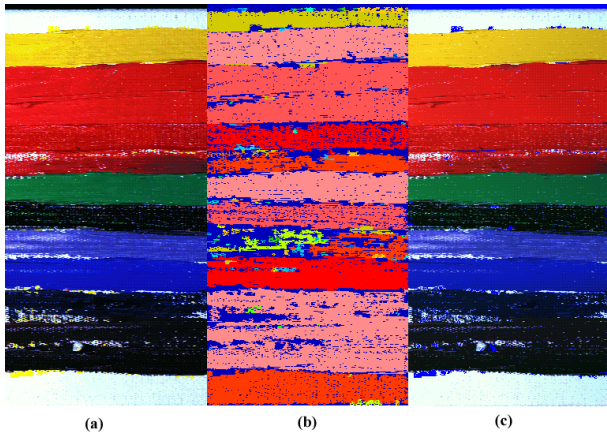


Figure 2. Segmentation of color range images of a painting: (a) 3-D view of the color range image,(c) segmented image regions, (d) reconstructed color range image.

- ical morphology*, 10th International Conference on Pattern Recognition, Atlantic City, 1990.
- [5] R.O. Duda, D. Nitzan, and P. Barret, *Use of range and reflectance data to find planar surface regions*, IEEE Trans. Pattern Analysis and Machine Intelligence, Vol. PAMI-1 no. 3, pp. 259–271, 1979.
- [6] B. Gil, A. Mitiche, and J.K. Aggarwal, J.K., *Experiments in combining intensity and range edge maps*, Computer Vision, Graphics, and Image Processing, Vol. 21 no. 3, pp. 395–411, 1983.
- [7] J.K. Hackett and M. Shah, *Segmentation using intensity and range data*, Optical Engineering, Vol. 28, no. 6, pp. 667–674, 1989.
- [8] T. Koezuka, Y. Kakinoki, Y. Suto, M. Nakashima, and T. Inagaki, *High-speed 3-D vision system using range and intensity images covering a wide area*, Application of Artificial Intelligence VII, Vol. SPIE-1095, pp. 1134–1141, 1989.
- [9] R.C. Luo and M.G. Kay, *Multisensor integration and fusion in intelligent systems*, IEEE Trans. on System, Man, and Cybernetics, Vol. SMC-19. no. 6, pp. 901–931, 1989.
- [10] F. Prieto, T. Redarce, P. Boulanger, and R. Lepage R., *Tolerance Control with high quality 3D data*, Third Conference on 3D Digital Imaging and Modeling, Quebec, Canada, May 28th-June 1st, 2001.
- [11] M. Rioux M., F. Blais F., J.A. Beraldin and P. Boulanger, *Range image sensors development at NRC laboratories*, Proc. of the Workshop on Interpretation of 3D Scenes, Austin, TX, November 27–29, 1989.
- [12] P.J. Rousseeuw and A.M. Leroy, *Robust regression and outlier detection*, J. Wiley and Sons, 1987.
- [13] H. Rushmeier and F. Bernardini, *Computing consistent normals and colors from photometric data*, 2nd International Conference on 3D Digital Imaging and Modeling (3DIM '99) October 4-8, 1999.

- [14] Y. Shirai, *3-D computer vision and applications*, IEEE International Conf. on Pattern Recognition, pp. 236–245, 1992.
- [15] I. Stamos and P. Allen, *Automatic registration of 2-D with 3-D imagery in urban environments*, Technical report, Dept. of Computing Science, Columbia, University, 2000.